Journal of Controlled Release 261 (2017) 216–222

Contents lists available at ScienceDirect

Journal of Controlled Release

journal homepage: www.elsevier.com/locate/jconrel

Tumor progression effects on drug vector access to tumor-associated capillary bed

Vaidotas Kiseliovas[a,b], Miljan Milosevic[c], Milos Kojic[a,c], Linas Mazutis[b], Megumi Kai[a], Yan Ting Liu[a], Kenji Yokoi[a], Mauro Ferrari[a], Arturas Ziemys[a,*]

[a] The Houston Methodist Research Institute, Houston, TX, USA
[b] Institute of Biotechnology, Vilnius University, Vilnius, Lithuania
[c] Research and Development Center for Bioengineering BioIRC, Kragujevac, Serbia

ARTICLE INFO

Keywords:
Metastatic tumors
Microfluidics
Drug delivery
Nanomedicine
Capillaries

ABSTRACT

Over the last decade, the benefits of drug vectors to treat cancer have been well recognized. However, drug delivery and vector distribution differences in tumor-associated capillary bed at different stages of disease progression are not well understood. To obtain further insights into drug vector distribution changes in vasculature during tumor progression, we combined intra-vital imaging of metastatic tumors in mice, microfluidics-based artificial tumor capillary models, and Computational Fluid Dynamics (CFD) modeling. Microfluidic and CFD circulation models were designed to mimic tumor progression by escalating flow complexity and chaoticity. We examined flow of 0.5 and 2 μm spherical particles, and tested the effects of hematocrit on particle local accessibility to flow area of capillary beds by co-circulating red blood cells (RBC). Results showed that tumor progression modulated drug vector distribution in tumor-associated capillaries. Both particles shared 80–90% common flow area, while 0.5 and 2 μm particles had 2–9% and 1–2% specific flow area, respectively. Interestingly, the effects of hematocrit on specific circulation area was opposite for 0.5 and 2 μm particles. Dysfunctional capillaries with no flow, a result of tumor progression, limited access to all particles, while diffusion was shown to be the only prevailing transport mechanism. In view of drug vector distribution in tumors, independent of formulation and other pharmacokinetic aspects, our results suggest that the evolution of tumor vasculature during progression may influence drug delivery efficiency. Therefore, optimized drug vectors will need to consider primary vs metastatic tumor setting, or early vs late stage metastatic disease, when undergoing vector design.

1. Introduction

Over the last few decades, cancer as a disease has been summarized into a set of fundamental hallmarks such as genomic instability, limitless replicative potential, evasion of apoptosis and growth suppression, angiogenesis induction, activation of invasion, and metastasis [1]. The tumor microenvironment plays a crucial role in several of the aforementioned characteristics that are also biologically highly heterogeneous. Within the same tumor, individual cells may have widely different geno- and phenotypes. On the other hand, tumors may recruit and associate with non-malignant cells, like pericytes, fibroblasts, macrophages, and neutrophils. Together, malignant and non-malignant cells constitute the tumor microenvironment and provide the necessary cytokines, growth factors, extracellular matrix and neovascular networks for nutrient delivery and waste removal for efficient tumor growth.

The hallmarks of cancer have been fully biologically established and validated for some time now, with therapies aimed at addressing genomic instability, apoptotic evasion, or angiogenesis. However, transport barriers and oncophysical origins have recently become important considerations for research and translational efforts, specifically with regards to drug delivery [2,3]. Drug delivery in cancer relies on the principle that drugs only work effectively against tumor cells if they are present there at sufficient quantities at the right time. However, delivery is a function of sequential obstacles such as systemic clearance, permeation of vascular wall, degradation of the drug itself, to name a few. Drug vectors help circumvent or reduce the effects of these obstacles by exploiting the enhanced permeability and retention (EPR) effect [4]. The EPR effect dictates that drug vectors of a certain size preferentially accumulate in tumors [5], with drug vector enrichment inside tumors enabling more efficient pharmacokinetics in tumor microenvironment. Our studies [6,7], as well as others' [8], suggest that

* Corresponding author.
E-mail address: aziemys@houstonmethodist.org (A. Ziemys).

http://dx.doi.org/10.1016/j.jconrel.2017.05.031
Received 9 January 2017; Received in revised form 18 May 2017; Accepted 26 May 2017
Available online 31 May 2017

tumor microenvironment-associated pharmacokinetics provides a better assessment of therapeutic efficacy of nanotherapeutics and drugs [6–8], while systemic pharmacokinetics alone may be insufficient [6,9–11]. However, recent studies have begun to recognize the complexity and heterogeneity of the EPR effect. Efficacy gains due to EPR are not universal, being more profound in murine models, and finding only limited gains in clinical settings [12–16]. We believe that a more enhanced understanding of local biodistribution of drugs and vectors will provide novel insights into the clinical utility of the EPR phenomena.

Capillaries associated with the tumor microenvironment are a crucial component of the EPR effect. The imbalance of anti- and pro-angiogenic factors, such as vascular endothelial growth factor (VEGF), leads to formation of immature, highly permeable, and abnormal vasculature that lacks smooth muscle cells and pericytes [17]. In addition to abnormal vasculature and lack of lymphatic drainage system, tumors exhibit high interstitial fluid pressure. High IFP poses a tremendous challenge for drug delivery that eliminates the convective flux in the tumor region and limits transport mechanisms to diffusion alone [18,19]. Moreover, in contrast to normal blood vessels that are well-organized hierarchical structures such as arterioles, venules and capillaries, tumor vascular networks have disorganized, chaotic architecture, where blood vessels are dilated and tortuous, as extensively illustrated by imaging several studies [20–22]. Growing tumors, either primary or secondary, remodel the tumor-associated vascular network making it tortuous and chaotic [22]. Given that this remodeling process is gradual, tumors of varying developmental stages may have different vasculature and potentially different EPR, which can affect nanotherapeutic drug delivery.

Despite intense basic and translational research in the areas of nanomedicine and drug delivery, the effects of tumor-associated microcirculation on drug vector distribution, especially during tumor progression, remain poorly understood. Herein, we sought to better understand how a gradual increase in tortuosity and chaoticity of capillaries during tumor progression alters the local distribution of drug vectors of different size. We employed microfluidics, intra-vital imaging (IVM) of mice tumors, and Computational Fluid Dynamics (CFD) to characterize flow and particle distribution. Findings from this study will lead to an enhanced understanding of differentials of local drug vector distribution at different tumor stages and will aid in the design and development of improved drug delivery strategies for metastatic tumors.

2. Materials and methods

2.1. Materials

Phosphate Buffered Saline (PBS), ethylenediaminetetraacetic acid (EDTA), Bovine Serum Albumin (BSA), fraction V were obtained from ThermoFisher Scientific. Carboxylate-modified polystyrene fluorescent (λ_{ex} = 575 nm; λ_{em} = 610 nm) latex beads of 0.5 and 2 μm size were purchased from Sigma Aldrich. The chosen particle sizes enable individual particle tracking, enabling for a more reliable analysis. The particle sizes and use of Rhodamine tracer covers the spectrum of vectors sizes, including the micron size [23]. Poly(dimethyl siloxane) (PDMS) was obtained from Dow Corning.

2.2. Red blood cell (RBC) preparation

Diagnostic RBCs were obtained from the Interstate blood bank, Memphis, USA. RBCs were diluted twice with PBS supplemented with 5 mg/mL BSA and 1 mM EDTA. 400 μL of diluted cells were layered on 300 μL of lymphocyte separation medium and centrifuged at 1200*g* for 15 min. After centrifugation, supernatant was discarded and the pellet was additionally washed 3 times with PBS containing 5 mg/mL BSA and 1 mM EDTA. We discarded all cell layers except RBCs, resulting in a pure RBC suspension. Finally, RBCs were suspended in PBS with various particles and used for flow experiments.

2.3. Cancer cell preparation

4T1 murine breast cancer cells were kindly provided by Dr. Isaiah J. Fidler (UT MD Anderson Cancer Center). Cells were cultured in high glucose DMEM supplemented 5% FBS, and antibiotics (100 units/mL penicillin and 100 μg/mL streptomycin) at 37 °C in a humidified atmosphere containing 5% CO_2. Cells were grown to 80% confluency, trypsinized with 3 ml of 0.25% trypsin 0.53 mM EDTA solution for 5 min at 37 °C until cells started to detach. Trypsin was quenched with 9 ml of media, and cells were then washed with 9 mL of PBS containing 5 mg/mL BSA and 1 mM EDTA. After washing of cells, cells were re-suspended in PBS containing BSA and RBC, where final 4 T1 cell concentration was ~0.5 × 10^6 cells/mL.

2.4. Flow experiments

Imaging of flow inside microfluidic capillaries was measured using an inverted fluorescent microscope system (Nikon eclipse Ti-U, Nikon) and 10× objective (S Plan Fluor ELWD 10× DIC NA 0.30, Nikon). Digital images were recorded with a digital CMOS camera (Orca flash 2.8, Hamamatsu) at 45 frames/s with 10 ms exposure time. Particles were diluted in PBS (supplemented with 1 mM EDTA and 5 mg/mL BSA) to a final concentration of 4 * 10^8 particles/mL. The solution was injected into a microfluidics device using a syringe pump (Harvard apparatus) at a flow rate of 0.1 μL/min. Prior to injection, the device was incubated for 2 h with PBS solution supplemented with 5 mg/mL BSA to reduce nonspecific particle adhesion. Each experiment was recorded for 60 s comprising 2725 frames (12-bit images). Prior to measurements, the flow was allowed to stabilized for 1 min. Recorded images were analyzed using the Fiji program [24].

2.5. Microfluidic capillary design and fabrication

Microfluidic devices were fabricated in PDMS using conventional soft lithography as described previously [25]. The design of a single microfluidic device is illustrated in Fig. 1 and consists of: i) inlet with passive filters, ii) capillary network (dashed box), and iii) outlet to collect fluids. Four capillary models, with sequentially escalated (c-I to c-IV) complexity and increased flow chaoticity were designed to mimic remodeling of capillaries in tumors and their microenvironment (Fig. 2). c-I design represents the simplest flow condition; c-II is a randomly modified c-I design by connecting adjacent flows; c-III is a modified c-II design having additional interconnections and dead-ends, where flow segments are lost; c-IV is a modified c-III design having

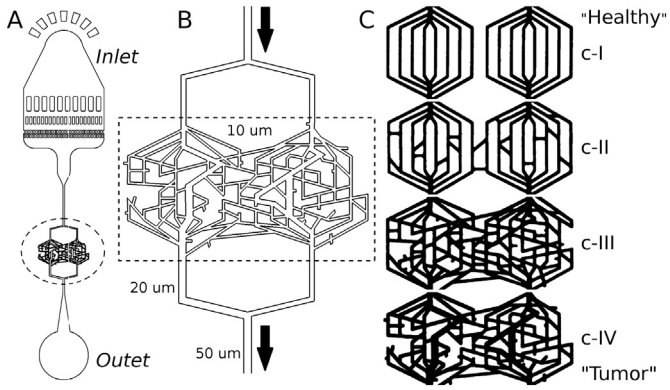

Fig. 1. Design of microfluidic capillaries. A. The design of the complete microfluidic device. B. The capillary network (c-III type) with characteristic widths of channels. C. Four microfluidic capillary networks (c-I, c-II, c-III and c-IV) capturing major differences of tumorigenesis.